

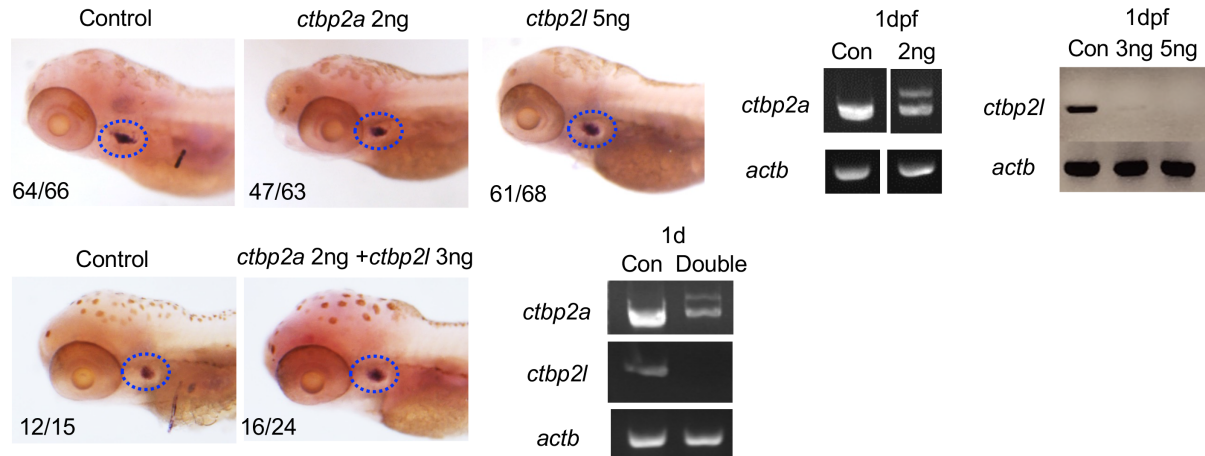
A

```

.....1130.....1140.....1150.....1160.....1170.....1180.....1190.....1200.....1210
Human_NP_0010773383.1 PWSVLDQQAHPFLNGATYRYPLWWEIDQQEIHPSVGVAPGGLPAAAMEGIIPGGIPVTHNLPVVAHPSQAPSPNQPTKHGNNREHPNEQ 456
Mouse_NP_034110.1 PWSVLDQQAHPFLNGATYRYP-----PGVGVAPGGLPAAAMEGIIPGGIPVTHNLPVVAHPSQAPSPNQPTKHGNNREHPNEQ 445
Zebrafish_ctbp2a_iso2 PWGVMEQ-QVHPFLNGGAYRVAQ-----PGAVSVSPGGMGQLEGMMPGGLPSAHPLPFGTQPSLAPSPFTQLLKHNDREHLAKS 444
Zebrafish_ctbp2a_iso1 PWGVMEQ-QVHPFLNGGAYRVAQ-----PLPAVSPGGMQDKMYT----- 1147
Zebrafish_ctbp1 PWGVMEQ-QVHPFLNGGAYRVAQ-----PLPAVSPGGMQDKMYT----- 860
consensus PW VmeQ VHPFLNGG YR i gv PGGL m

```

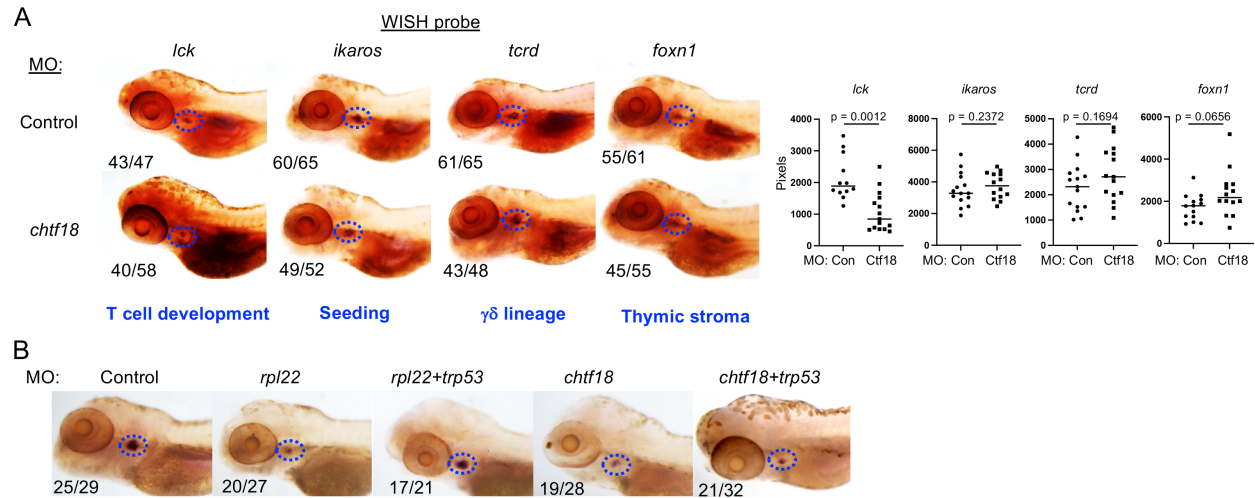
B



**Supplemental Figure 1. Analysis of candidate patient variant, CTBP2.** (A) Sequence alignment of human, mouse and zebrafish CTBP2 paralogues. The human de novo D437N mutation and in frame 11 amino acid insertion are indicated by red square outline (B). *ctbp2* knockdown does not block T cell development. Zebrafish embryos were injected with MO designed to block splicing of *ctbp2a* E516 (2ng) and *ctbp2l* E111 (5ng) alone or in combination (2 and 3 ng, respectively). MO efficacy was verified by RT-PCR at 1dpf. The impact on T cell development was assessed by WISH using an *lck* probe at 5dpf. Thymus is indicated by dashed blue ovals.

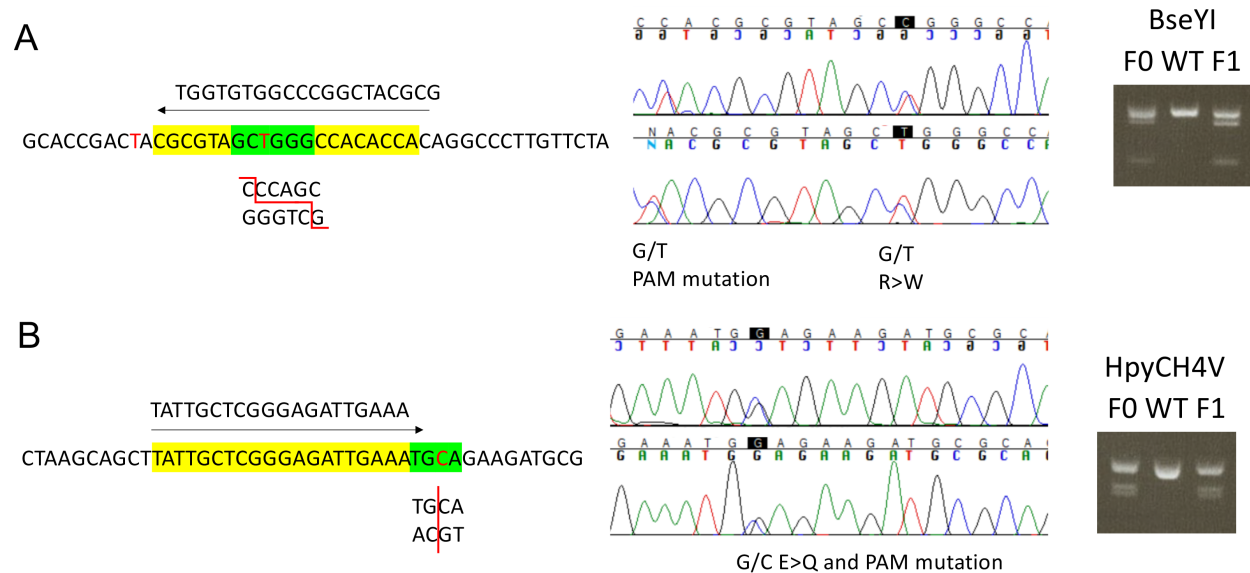
Zebrafish	YFPFLPAAFHQLYAATSVPRINYPHSHYEAFTKTQHIRNALLAMLNDIPPAIQSRVCMSS
Human	YPPFLPVAFHVLFASSHTPRITFPSSQQEAQNRMSQMRNLIQTLVSGIAPATRSRATPQA
Mouse	YLPFVPAAFHVLFASSHVPRIITFPSSQQEAQTRMSQTRNHIQTLVSGMAPTTRS
	* **:*.*** *:*: .***.* *: ** .: .: ** : :*: .: *: **: .:
Zebrafish	LCLDILSLLLELISPKLRVNPQLYSTREKQQLYDLIDTMINYNLTQRDRTPEGQYTYV
Human	LLLDALCLLLDILAPKLRVSTQLYSTREKQQLASLVGTMLAYSLTYRQERTPDGQYIYR
Mouse	LVLDTLCLLLDVLAPKLRVSTQLYSAHEKQQLSCLVGTMLAYSLTYHQERTPDGQYLYK
	* ** *.***:***.***:*** * :.***: *.***:***:*** *
Zebrafish	LEPNIEDVVNYPGLPPRRQLTYQVKQLIARETEIRMRRAVERAQSRNPQKMETVNKNQ-
Human	LEPNVEELCRFPELPARKPLTYQTKQLIAREIEVEKMRRAEASARVENSPPQVDGSPGLE
Mouse	LEPNVEEVCRFPELPARKPLTYQAKQLIAREIEVEKMRRAEALAWARSGPQVDQSSGPA
	*****:*: .:* ** *: ****.***** *:***.* .. :*: .
Zebrafish	----EEKKTEVKKQTSRHHQORLENIVKQTVVETRPDLDFFGRAIVPKEKPVVTATSEDG
Human	GLLGIGIEKGVHRPAPRNHEQRLEHIMRRAAREEQPEKDFFGRVVVRSTAVPSAGDTAPE
Mouse	SLWTDSGEKGTRQPVPRNHEQRLEHIMTRATVQEPPERDFFGRVVIRKVAVPSREVEAPQ
	:. .: . ***:***:*. :. : :** *****.:. .
Zebrafish	KVSGVLNIGKAVGNSDVWFRFNEGVSNAVRRNVYIRELL
Human	QDSVERRMGTAVGRSEVWFRFNEGVSNAVRRSLYIRDLL
Mouse	KDADEWRMGVAVGRSEVWFRFNEGVSNAVRRSLYIRDLL
	: : .:* ***.***:*****.***:***:***

**Supplemental Figure 2. Sequence alignment of *CHTF18* orthologs.** Full length human, mouse and zebrafish *CHTF18* were aligned using ClustalX. Conservation across the sequences is indicated (identical-\*, highly similar-:, similar-.) with the conserved patient variant amino acids boxed in red.



**Supplemental Figure 3. Analysis of distinct thymic cell subsets in *chtf18* morphants. (A)**

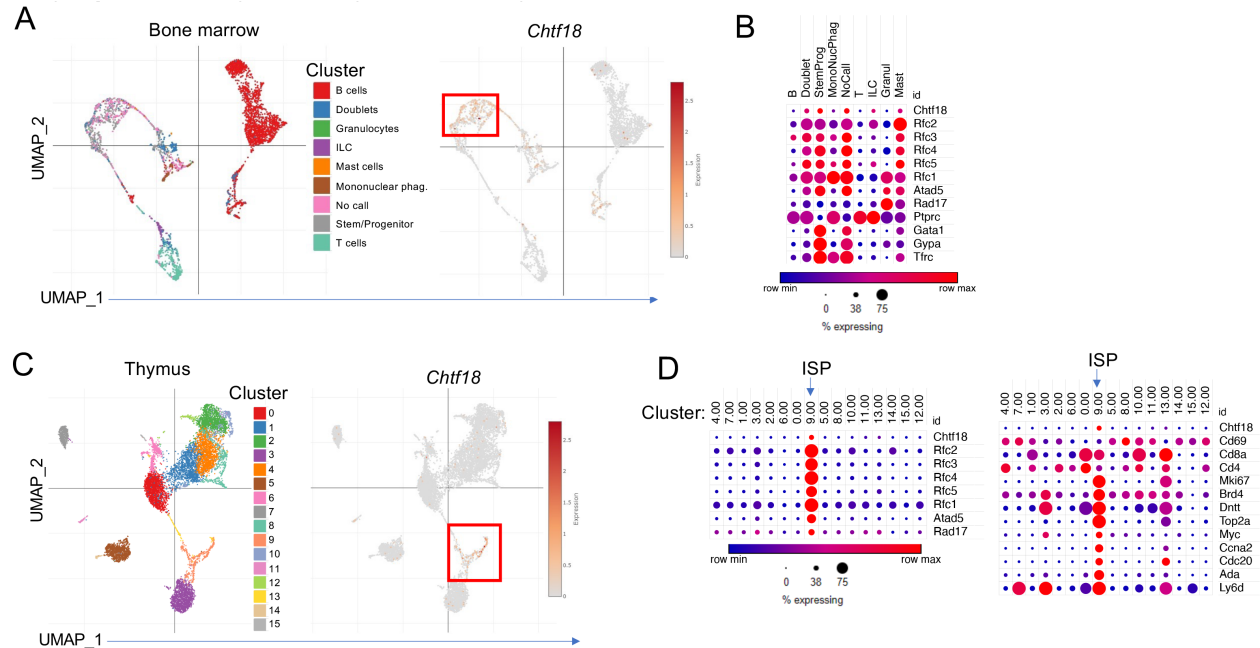
The effect of *chtf18* knockdown on development of:  $\alpha\beta$  T cells, *lck*; seeding progenitors, *ikaros*;  $\gamma\delta$  T cells, *tcrd*; and thymic stroma, *foxn1*. WISH signals were quantified using Image J and depicted graphically. Statistical significance was evaluated using two way ANOVA. p values are indicated on graphs. **(B)** The dependence of the developmental arrest in *chtf18* morphants on p53 was assessed by knocking down *Trp53* using splice site MO. *Rpl22* served as a positive control. The impact of T cell development was assessed by *lck* WISH and the thymus is marked by dashed blue ovals. The frequencies of embryos with the depicted staining pattern are indicated on the images.



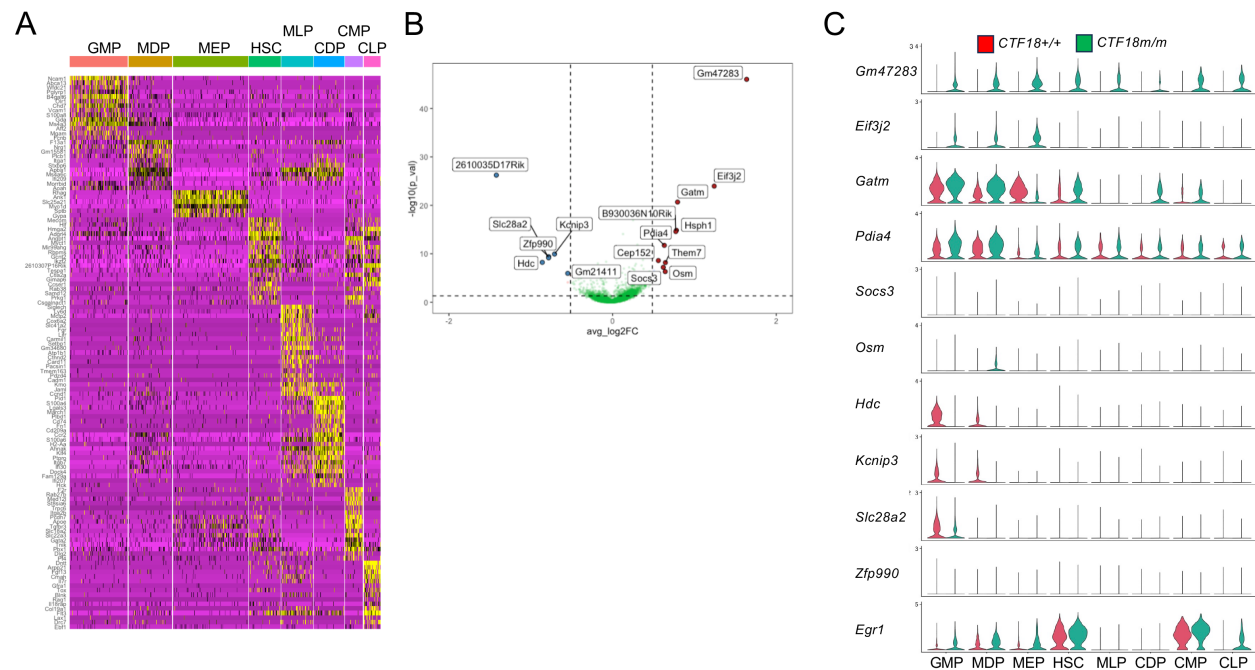
**Supplemental Figure 4. Generation and sequence validation of *Chtf18* mutant mice. (A, B).**

Mice bearing mutations equivalent to the patient variants *Chtf18*R745W (**A**) and *Chtf18*E845Q (**B**) were produced by CRISPR mediated gene editing. sgRNA target sequences are shown with the sgRNA sequence indicated, its target region highlighted in yellow, mutations in red, and newly created restriction enzyme sites indicated in green. Sequence trace files showing the protospacer adjacent motif (PAM) mutation and specific coding mutation are depicted, as are the restriction digests employed for typing founder (F0) and progeny (F1) tail DNA.



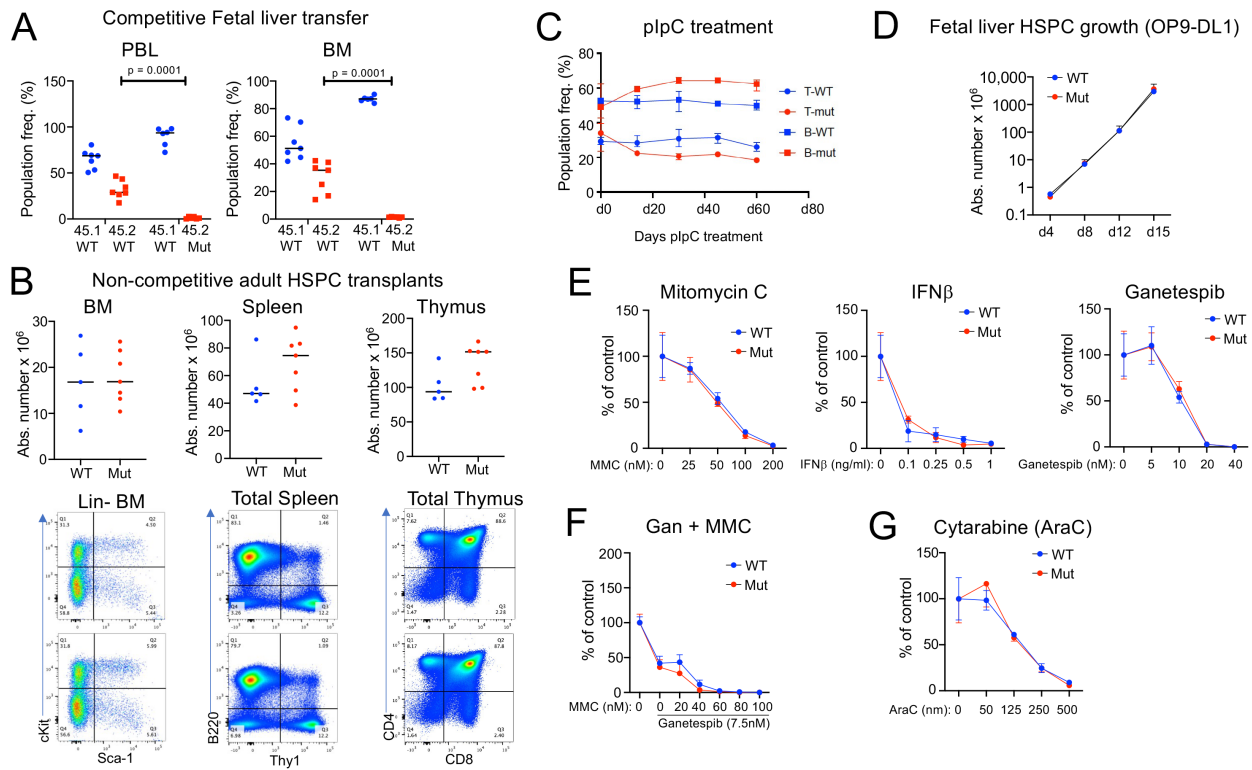


**Supplemental Figure 5. *Chtf18* expression in thymus and bone marrow progenitors by public scRNA-Seq data.** (A) (left) UMAP plot of 9 clusters resulting from publicly available scRNA-Seq analysis of adult C57BL/6 mouse bone marrow (3865 cells). (right) *Chtf18* expression mapped onto the UMAP coordinates within the clusters with white to deep red indicating expression. (B) Bubble plot of the scaled expression of clamp loader and lineage specific factors in each cluster with minimum expression shown in blue and maximum in red. Bubble size indicates the percentage of cells in each cluster expressing the factor. (C) (left) UMAP plot of 16 clusters resulting from publicly available scRNA-Seq analysis of adult C57BL/6 mouse thymus (10,741 cells). (right) *Chtf18* expression mapped onto the UMAP coordinates within the clusters with white to deep red indicating expression. (D) Bubble plot of the scaled expression of clamp loader and lineage specific factors in each cluster with minimum expression shown in blue and maximum in red. Bubble size indicates the percentage of cells in each cluster expressing the factor.



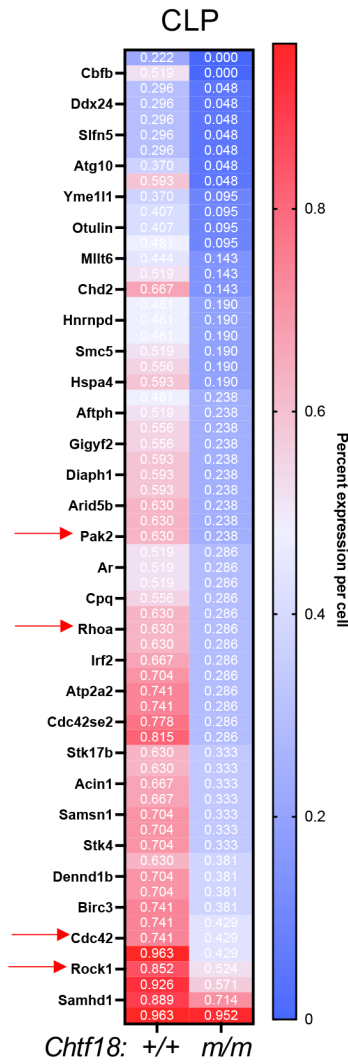
**Supplemental Figure 6. scRNA-Seq analysis of *Chtf18* mut HSPC.**

A) Heatmap of the top differentially expressed genes in each of the eight HSPC clusters in *Chtf18* mut mice. B) Volcano plot of the top differentially expressed genes between *Chtf18* wildtype and mut HSC/MPP cluster. C) Violin plot representation showing gene expression levels of the top upregulated genes across all eight clusters in *Chtf18* WT and mut HSPCs.



**Supplemental Figure 7. Function of adult and fetal *Chtf18* mut HSPC. (A).** The ability of day 14.5 FL HSPC from WT and *Chtf18* mut mice (CD45.2) to repopulate hematopoiesis was assessed by competitive transplantation using allotype marked (CD45.1) competitor. 100,000 HSPC from CD45.2 WT or *Chtf18* mut mice were mixed with an equal quantity of CD45.1 competitor cells and transferred into irradiated recipients. After 6 weeks, the hematopoietic reconstitution was assessed on peripheral blood lymphocytes (PBL) and on explanted bone marrow cell suspensions by flow cytometry using anti-CD45.1 and anti-CD45.2 antibodies. Cell frequencies were displayed graphically as scatter plots. Statistical significance was assessed by two-way ANOVA. **(B).** The ability of 100,000 adult WT and *Chtf18* mut HSPC (CD45.2) to repopulate hematopoiesis upon transfer to irradiated (CD45.1) recipients in a non-competitive setting was assessed on the indicated explanted tissues by flow cytometry after 6 weeks. Cell frequencies were displayed graphically as scatter plots. Statistical significance was assessed by two-way ANOVA. **(C).** The capacity of WT and *Chtf18* mutant HSPC to withstand repeated cycles of inflammation-induced activation was assessed by serial treatment with plpC. The mice were dosed with 15mg/kg plpC two times per week for 60 days and the impact on lymphopoiesis was assessed by flow cytometry on PBL at the indicated time points. Statistical significance was

assessed by two-way ANOVA. **(D-G)** The growth of WT and *Chtf18* mut FL precursors on OP9-DL1 monolayers **(D)** and their ability to withstand treatment with **(E-F)** interferon- $\beta$ , DNA-damaging agents (Mitomycin C), a HSP90 inhibitor (Ganetespib), and **(G)** Cytarabine was assessed on triplicate cultures after 4d by cell counting. Results of dose-response analysis were depicted graphically. Statistical significance was assessed by multiple unpaired t tests.



**Supplemental Figure 8. Impact of *Chtf18* mutations on gene expression in CLP.** A heat map of genes differentially expressed in CLP is depicted. Rho family GTPases and their regulators are denoted by red arrows.